OFFSHORE TECHNOLOGY CONFERENCE
6200 North Central Expressway
Dallas, Texas 75206

PAPER
NUMBER OTC 1621

THIS IS A PREPRINT --- SUBJECT TO CORRECTION

Fundamental Study of Underwater Welding

By

Alan J. Brown, James A. Staub and Koichi Masubuchi,
Massachusetts Institute of Technology

ABSTRACT

This paper stresses the need for a reliable underwater "wet" welding process and points out the value of fundamental research in this area. Various heat transfer mechanisms are sited as being ultimately responsible for metallurgical structure and residual stress. A finite element heat transfer model including radiation, boiling and the arc bubble mechanism is described. Results are evaluated in relation to individual phenomena and areas for future research are defined.

INTRODUCTION

The need for a reliable underwater joining process is very real in today's offshore technology. Although underwater chamber welding "in the dry" has proven to be a partial solution to the problem, this process is limited to the welding of regular shapes, such as pipelines and is very expensive. For more general underwater repairs and fabrication chambers are impractical and welding "in the wet" is desirable. The only other alternatives for such work are prefabrication and dry-docking, but complete prefabrication is not always possible and dry-docking is costly.

Unfortunately the "state-of-the-art" in underwater wet welding has advanced very little since World War II and for this reason its use has been limited to temporary repair and salvage work. The standard U. S. Navy rule of thumb for wet underwater welds predicts 80% strength and 50% ductility when compared to similar surface welds. Before the use of underwater welding can be expanded to permanent repairs and structural fabrication present methods must be modified or radically changed.

There are two basic approaches to select from when solving such a problem:

References and illustrations at end of paper.

1. Conduct an empirical study in which proposed processes might be tested, optimized, and evaluated. This first requires a proposed process to test.
2. Conduct a fundamental study in which the various arc, heat, metallurgical and physical phenomena may be analyzed and modeled. An understanding of these phenomena could then be used in more rational selection and development of new processes.

We have chosen to undertake the second of these approaches combined with an empirical study sufficient to substantiate our mathematical models. Such work is particularly compatible to the university whereas development of hardware and technique might best be done in industry.

GENERAL ASPECTS OF UNDERWATER ARC WELDING

The process currently used in nearly 100% of all underwater wet welding in this country is the shielded metal arc process or stick electrode welding. The underwater process is very similar to that used on the surface. An arc is formed between the tip of a consumable metal electrode and the grounded work piece. Filler metal is provided by the melting electrode which is manipulated by a diver. The arc is sustained in a high temperature plasma which is surrounded by a gaseous bubble. Due to the abundance of H_2O, the plasma may contain 90% ionized hydrogen, and the bubble varying amounts of H_2, O_2, N_2, CO_2, steam and various trace elements. Slow burning coatings on the electrodes allow a drag manipulation technique to be used. The standard electrode in use is a 5/32 inch diameter or 3/16 inch diameter E6013 or equivalent, although recent research indicates improved weld quality with iron powder electrodes.

Recent work by E. A. Silva at the University of California has introduced the "shroud technique" to underwater welding. This method encloses the arc in a plexiglass dome through which the electrode is passed. This dome is dragged along with the electrode and serves to hold the evolved gases in the vicinity of the arc.

An underwater gas metal arc process has been used in the Soviet Union. In this process shielding gas is fed around the arc. This gas serves to force back the surrounding water, but the effect of this is not known.

We are currently studying each of these processes in an attempt to determine their basic phenomena. Our goal is to understand these fundamental mechanisms so that this knowledge may be taken and used in the development of a single more workable process.

THE HEAT TRANSFER

Overview

Of prime consideration with any welding process are its thermal characteristics. They are ultimately responsible for metallurgical structure and residual stress. Understanding these characteristics will make rational selection and development of new processes a more reasonable task.

Due to the water environment envolved in underwater welding, cooling is rapid and steep temperature gradients during welding are unavoidable. A great breakthrough in surface welding research came with Rosenthal's work in the late 30's on plate temperature distribution during welding. Rosenthal assumed that the welding arc was a point source of heat, moving in a straight line. This approximation is valid away from the weld, but is poor in close, making it of little use with underwater welding where temperature may drop off to ambient at a distance of 1/2 inch from the weld center line. Another method of analysis had to be considered.

After transients have settled out the moving arc is surrounded by a quasi-static temperature distribution which produces a corresponding quasi-static solid and liquid region in the plate. (See Figure 1.) The liquid region is a small area directly around the source where heat transfer takes place via a complicated combination of convection, conduction, melting, and fusion. Recent work at the University of Wisconsin introduced a finite difference numerical procedure for determining the

temperature distribution in thin plates welded on the surface. This work is being modified at M.I.T. for use with underwater welding. The advantage of this method is that it uses the location of the melting isotherm as a boundary condition thus overcoming problems encountered with the point source method.

Four basic tasks are envolved in formulating the heat transfer model:

1. Setting up the basic partial differential equation
2. Identifying all source and loss terms
3. Mathematically defining the boundary conditions
4. Numerically solving the problem.

Each of these will be discussed briefly in the next few sections.

The Basic Equation

This entire analysis is based on the energy equation in two dimensions with source terms:

$$\frac{\partial}{\partial x}(\kappa\frac{\partial T}{\partial x}) + \frac{\partial}{\partial y}(\kappa\frac{\partial T}{\partial y}) + w_i = \rho C_p \frac{\partial T}{\partial t} \quad (1)$$

Putting this into correct form for quasi-steady state and nondimensionalizing yields:

$$\frac{\partial^2 T^*}{\partial \zeta^{*2}} + \frac{\partial^2 T^*}{\partial y^{*2}} + \frac{\partial \log\kappa}{\partial T^*}\left[\left(\frac{\partial T^*}{\partial \zeta^*}\right)^2 + \left(\frac{\partial T^*}{\partial y^*}\right)^2\right] + \frac{\dot{q} x_o^2}{\kappa L (T_M - T_\infty)} = -\frac{V}{\alpha x_o}\frac{\partial T^*}{\partial \zeta^*} \quad (2)$$

$$\zeta^* = \frac{\zeta}{x_o} \qquad \zeta = x - Vt$$

$$y^* = \frac{y}{x_o} \qquad T^* = \frac{T - T_\infty}{T_M - T_\infty}$$

This equation forms the basis for all remaining calculations.

Source and Loss Terms

Keeping track of all the energy emitted by the welding arc is a difficult problem, one which even for surface welding has not been completely solved. In our early work we made the assumption that all energy entering into the solid portion of the plate passed through the isotherm of melting. Computer runs of this model indicate that this may be a poor assumption. This will be discussed in more detail later, but to summarize, it now seems apparent that spread heat or a preheating-post heating effect takes place in spite of the surrounding water. The nature and distribution of this heat is a problem remaining to be solved. In this model joule or plate resistance heating and convection effects are also assumed negligible.

The greatest heat losses underwater are from boiling and radiation. Due to the complexity of boiling heat transfer its phenomena are normally subdivided into distinct regimes, each having its own mathematical model. (See Figure 2.)

As the temperature of the plate is increased above the saturation temperature bubbles begin to form on its surface. The bubble formation stirs up the water near the surface of the plate and increases the heat transfer. During the transition phase these bubbles begin to come together forming an unstable film which reduces the heat transfer. Finally, a stable film forms which limits the bulk of the heat transfer to radiation.

For ease in computer calculations the nucleation regime was approximated to end at 300° F and transition at 500° F.

The Rohsenow correlation for nucleate boiling after substituting appropriate constants and normalizing yields:

$$\dot{q}_{nucleate} = 1.75[T^*(T_M - T_\infty) + T_\infty - T_{SAT}]^3 \frac{Btu}{hr\text{-}ft^2} \quad (3)$$

In the film boiling regime, Berenson gives a relation for horizontal flat plates which after similar reduction yields:

$$\dot{q}_{film} = 190[T^*(T_M - T_\infty)]^{.75} \frac{Btu}{hr\text{-}ft^2} \quad (4)$$

Connecting these two regimes is the transition regime whose correlating function has the form:

$$\dot{q}_{transition} = M(T - T_{SAT})^b \frac{Btu}{ft^2\text{-}hr} \quad (5)$$

With the two boundary conditions:

$$\begin{aligned} &1.\ q_T = q_N \text{ at } T = 300^\circ F \\ &2.\ q_T = q_F \text{ at } T = 500^\circ F \end{aligned} \quad (6)$$

M and b may be evaluated.

Again in our original model, it was assumed that the plate temperature was solely responsible for its own heat transfer. However, bubble or gas phenomena around the arc limits what might be some form of boiling to only radiation by forming a protective pocket over a portion of the plate and thus reduces the heat transfer. A solution to this problem lies in modeling the dynamics of the bubble or gas as they relate to the heat transfer.

The final heat loss is that due to radiation. The electrical analogy for this radiation mechanism is shown in Figure 3 and yields:

$$\dot{q}_{radiation} = \frac{(T^4 - T_{WATER}^4)}{\frac{1}{e_p} + \frac{1}{e_w} - 1} \frac{Btu}{hr\text{-}ft^2} \quad (7)$$

Assuming that the steel plate ($e_p = .8$) is radiating into water ($e_w = .95$) whose temperature is approximately at the saturation temperature and normalizing yields:

$$\dot{q}_{radiation} = 1.317 \times 10^{-9}\{[T^*(T_M - T_\infty) + T_\infty]^4 - T_{SAT}^4\} \frac{Btu}{ft^2\text{-}hr} \quad (8)$$

In this model it is assumed that the plate emissivity is that for the solid phase. In future models consideration will be made for the effect of near-molten temperatures on the emissivity.

The Boundary Conditions

The heat transfer taking place in the plate is bounded on two sides. The isotherm of melting serves as the interior boundary and is defined as the interface between solid and liquid phase, assumed to be at the melting temperature. The exterior boundary is assumed to be at ambient water temperature.

Predicting the location of the pool contour analytically requires the use of a temperature model, but such a model is precisely what we do not have. Point source theory predicts egg-shaped contours, quite unlike the observed tear-drop shape. For these reasons reliance on entirely analytical methods is ruled out. Second best to an entirely analytical approach is analytical correlation of empirical data. This was done using Rosenthal's point source temperature equation:

$$T - T_\infty = \frac{\dot{Q}}{L} \frac{1}{2\pi\bar{\kappa}} e^{-(\bar{\lambda}V)\zeta} K_o(\bar{\lambda}Vr) \quad (9)$$

$$r = \sqrt{\zeta^2 + y^2}$$

$$\dot{Q} = 3.415\eta EI \frac{Btu}{Hr.}$$

Assuming the heat content per unit pool area to be:

$$H_m = \bar{C}_p\bar{\rho}(T_M - T_o) \frac{Btu}{ft^2} \quad (10)$$

and nondimensionalizing yields:

$$T^* = p^*\eta e^{-\zeta^*} K_o(r^*) \quad (11)$$

$$p^* = \frac{3.415EI}{2\pi\bar{\alpha}LH_m}$$

$$\zeta^* = \bar{\lambda}V\zeta \qquad r^* = \bar{\lambda}Vr$$

Next, it is necessary to consider the geometry of the molten pool. (See Figure 4.) At the maximum pool width:

$$\left(\frac{\partial T^*}{\partial \zeta^*}\right) = 0 \qquad (12)$$

which yields:

$$p^* \eta e^{-\zeta_w^*} \left[-K_o(r_m^*) - K_1(r_m^*)\frac{\zeta_w^*}{r_m^*}\right] = 0$$

or

$$\zeta_w^* = -r_m^* \frac{K_o(r_m^*)}{K_1(r_m^*)} \qquad (13)$$

Also since this contour is at the melting temperature:

$$T^* = 1 = p^* \eta e^{-\zeta_m^*} K_o(r_m^*)$$

or

$$p^* = \frac{\exp\left[-r_m^* \frac{K_o(r_m^*)}{K_1(r_m^*)}\right]}{\eta K_o(r_m^*)} \qquad (14)$$

This equation is very significant in that it relates the radius at maximum width to a single welding parameter and an efficiency which can be assumed constant for a given process. Maximum width and length can then be expressed in terms of this radius:

$$y_{max}^* = 2r_m^* \left[1 - \left(\frac{K_o(r_m^*)}{K_1(r_m^*)}\right)^2\right]^{1/2} \qquad (15)$$

$$x_{max}^* = 2r_m^* \frac{K_o(r_m^*)}{K_1(r_m^*)} \ln(\eta) \qquad (16)$$

These equations may be used to correlate the empirical data. Pool dimensions were determined by using a high pressure blast of argon to blow out the pool at the completion of an underwater welding run. Data from the first set of runs was very scattered due to difficulty in blowing out underwater, but results yielded

$$x_{max}^* = 4.42\, p^{*1.01} \qquad (17)$$

$$y_{max}^* = 3.16\, p^{*.67} \qquad (18)$$

For use in the temperature model, a contour must be fitted to the three maxima points. (See Figure 5.) For this purpose it can be assumed that:

1. $\frac{\partial y^*}{\partial \zeta^*} = 0$ at the tail of the teardrop shape.

2. $\frac{\partial y^*}{\partial \zeta^*} = \infty$ at the head of the teardrop shape.

This curve was fitted with the equation

$$y^2 = Bx^a(X_m - x)^b \qquad (19)$$

where

$$B = \frac{(Y_{m/2})^2 (a+b)^{a+b}}{(aX_m)^a (bX_m)^b}$$

This is plotted along with the typical contour in Figure 5. Given the contour equation it is possible to lay out a grid network and use intersecting points as the interior boundary condition.

Numerical Solution

The energy equation with source terms and boundary conditions is ultimately solved numerically on an IBM 360 computer using the G compiler. Before this can be done, however, the energy equation and boundary conditions must be put into form suitable for such solution. This is done as follows:

1. The shape of the pool contour is generated from the lumped parameter, p^*.
2. A grid computational block is layed out along with contour intersections. (See Figure 4.)

3. Each node on this block is assigned an initial temperature using Rosenthal's temperature equation (9).

4. Finally, an iterative finite difference solution is carried out.

The finite difference technique uses the difference in temperature between predetermined grid nodes to approximately define temperature derivatives. Substituting these into the normalized temperature equation allows the temperature at a given point to be determined from that of surrounding points using a Gauss-Siedel iterative procedure. This involves using the latest temperatures as they become available in a systematic scanning of mesh points, beginning at the interior boundary.

Using the gird shown in Figure 5 temperatures T_1, T_2, T_3, and T_4 may be approximated in terms of T_o and the grid spacing using Taylor series:

$$T_1 = T_o + S_1 \frac{\partial T}{\partial x} + \frac{S_1^2}{2} \frac{\partial^2 T}{\partial x^2}$$

$$T_2 = T_o - S_2 \frac{\partial T}{\partial x} + \frac{S_2^2}{2} \frac{\partial^2 T}{\partial x^2} \qquad (20)$$

$$T_3 = T_o + S_3 \frac{\partial T}{\partial y} + \frac{S_3^2}{2} \frac{\partial^2 T}{\partial y^2}$$

$$T_4 = T_o - S_4 \frac{\partial T}{\partial y} + \frac{S_4^2}{2} \frac{\partial^2 T}{\partial y^2}$$

Combining these equations with the energy equation allows T_o to be expressed in terms of these temperatures and the grid spacing.

The Empirical Study

In order to test the validity of the heat transfer model temperature measurements were taken while welding underwater. Chromal-Alumal thermocouples were mounted and waterproofed in mild steel plates. Welding beads were then run with these thermocouples at various distances from the weld centerline and the resulting temperature histories were recorded. (See Figure 6.)

In this study, 1/8 inch mild steel plates and E6013 Electrodes were used. Welding currents ranged from 150 to 250 amps and all welding was horizontal in about 6 inches of water. This technique allowed the electrode holder to be kept dry by having only the electrode penetrate the surface.

Most critical in these experiments was achieving truly two-dimensional welds, welds which did not vary appreciably in width over the thin cross-section of the plate. This requirement limits the range of welding currents and speeds that can be used.

Results

Typical computer versus actual temperature histories are shown in Figure 7. This graph represents the quasi-static temperature distribution along a line parallel and y inches away from the weld centerline, x = 0, being the origin or arc location. The dimensionless distance and time may be transformed as follows:

$$T = 2655T^* + 45° \quad °F$$

$$x = x^*/41 \text{ inch} \qquad (21)$$

Pictured in this graph are the empirical and computed temperature histories from an underwater welding run along with the results of a similar run done in air.

In analyzing these graphs the reader should notice three major characteristics:

1. The peak temperatures predicted by the model were in very good agreement with the measured temperatures. Slight overshooting might be due to the speed of response and accuracy of the thermocouples at high temperatures.

2. The length of the temperature cycle was also predicted with fair accuracy by the model.

3. The predicted cooling curve, on the other hand, was far too rapid indicating a gross overestimate of the heat transfer in this region. (See Figure 8)

BUBBLE AND GAS PHENOMENA

Discussed as thermal phenomena were mechanisms taking place due to and consequently controlling the temperature distribution in the plate. Independent of these mechanisms are various physical phenomena taking place above the plate. The arc bubble and trapped or impinging gases can affect the heat transfer taking place at the top of the plate. The mechanisms envolved in these phenomena as they relate to the heat transfer are our present concern.

A high speed motion picture study is in progress and early runs with the shielded metal arc process show an arc bubble mechanism as pictured in Figure 9. The critical features to be noticed in this diagram are:

1. The bubble at break-away consists of a nearly spherical upper portion which remains after the sphere has detached.
2. A minimum bubble size equal to the residual hemisphere always encloses the arc.
3. Minimum contact radius for this hemisphere at a 6-inch water depth is .25 to .35 inches and appears to be fairly invarient with changes in welding speed and arc current.
4. The maximum radius of the spherical portion is .4 to .5 inch.
5. Gas evolution rates are on the order of 40 cc/sec with E6013 electrodes. This figure also was relatively stable with changes in current and speed.
6. Bubble production has a frequency of 14 to 16 bubbles per second.

This experiment was conducted in 6 inches of water, using E6013 electrodes, various arc currents and speeds, and using the HiCam camera with 16 mm high speed ektachrome film.

The dynamics of a welding shroud or impinging gases are currently under study.

CONCLUSION

In concluding one must remember that the true value of this research is not the production of an efficient temperature-predicting model, but the understanding obtained concerning the various phenomena taking place in an underwater welding process. This understanding is gained through the analysis, use, and manipulation of such a model.

The phenomena considered in the original model can be summarized as follows:

1. The moving arc produces a quasi-static temperature distribution which can be represented by the appropriate energy equation with source terms.
2. The arc pool contour is assumed to be the only source of energy in the plate and serves as the interior boundary.
3. Boiling and radiation account for the major heat losses and they may be modeled by appropriate equations in terms of the plate temperature.
4. Pool dimensions and shape can be correlated with a lumped welding parameter.

Characteristics of the resulting temperature history then leads to certain conclusions, additions, and modifications of this model. The over-rapid cooling curve indicates the following necessary changes:

1. The spread-heat input must be determined and added as an additional energy source.

2. Although the boiling equation presented is quite valid for the top side of a plate it has been concluded that a different model is necessary for the bottom. Bubble buoyancy should act to stabilize a film sooner and thereby reduce the heat loss.
3. Bubble and gas phenomena on top of the plate would act to eliminate sizeable boiling heat transfer in this region.

A better understanding of these mechanisms will permit the development of a more efficient underwater joining process and ultimately this is our goal.

NOMENCLATURE

C_p	specific heat (Btu/lbm. °F)
E	machine voltage (V)
e	emissivity (Btu/hr-ft^2)
I	machine current (amps)
K_o, K_1	Bessel functions
L	plate thickness (ft)
P,B,a,b,	pool correlation parameters
$\dot{Q}$	energy input from machine (Btu/hr)
$\dot{q}$	heat transfer rate (Btu/ft^2-hr)
r_m	radius at maximum width of weld pool
S	finite difference grid spacing
T	plate temperature (°F)
T_o, T_{SAT}, T_M	ambient, water saturation, plate melting temperatures (°F)
V	welding speed (ft/hr)
x	distance in direction parallel to weld bead (ft)
X_o	characteristic length (ft)
X_{max}, Y_{max}	maximum length and width of weld pool
w_i	volume source term (Btu/ft^3-hr)
α	thermal diffusivity (ft^2/hr)
λ	average reciprocal diffusivity (hr/ft^2)
κ	thermal conductivity (Btu/hr.ft.°F)
η	percent of machine energy transferred to pool
ρ	density of steel (lbm/ft^3)
σ	Stefan-Boltzmann constant (Btu/ft^{2}hr. °R^4)
ζ	quasi-static x coordinate (ft)
*	indicates nondimensional variable

REFERENCES

Pavelec, V., Temperature Histories in Thin Steel Plate Welded with Tungsten Inert Gas, Ph.D. Thesis, University of Wisconsin, 1968

Silva, E. A., Shielded Metal-Arc Welding Underwater, Welding Journal, p. 406, June, 1971

Staub, James, Temperature Distribution in Thin Plates Welded Underwater, Naval Engineer's Thesis, M.I.T., 1971

Masubuchi, K., A Condensed Report on Underwater Cutting and Welding State-of-the-Art, Appendix to Materials for Ocean Engineering, M.I.T. Press, May, 1970

Brown, A., Methods of Research in Underwater Welding, Department of Naval Architecture and Marine Engineering, M.I.T., June, 1971

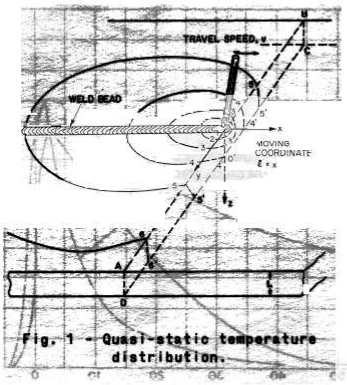

Fig. 1 - Quasi-static temperature distribution.

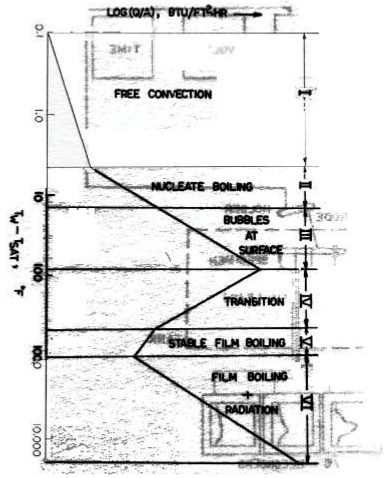

Fig. 2 - Characteristic boiling curve.

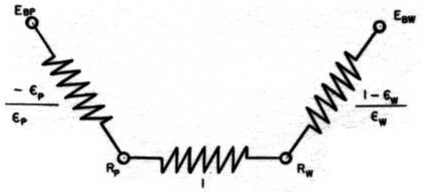

Fig. 3 - Radiation circuit analogy.

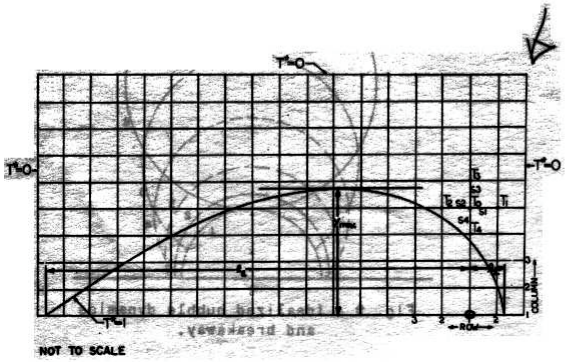

ig. 4 - Computational block.

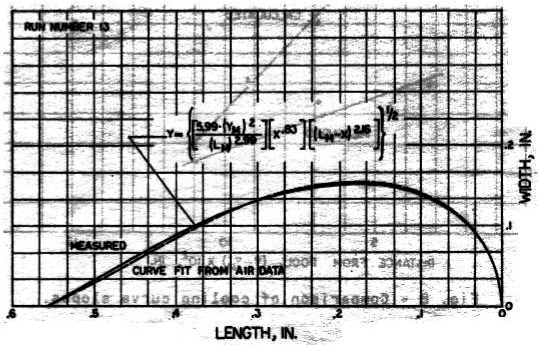

Fig. 5 - Pool contour

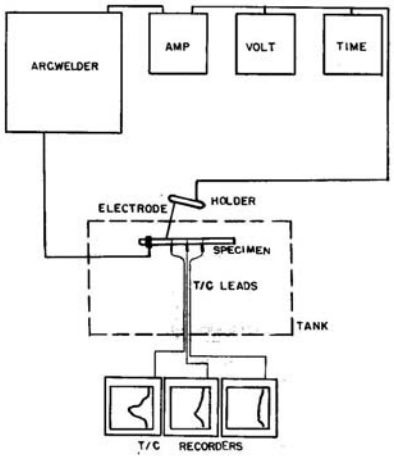

Fig. 6 - Apparatus schematic.

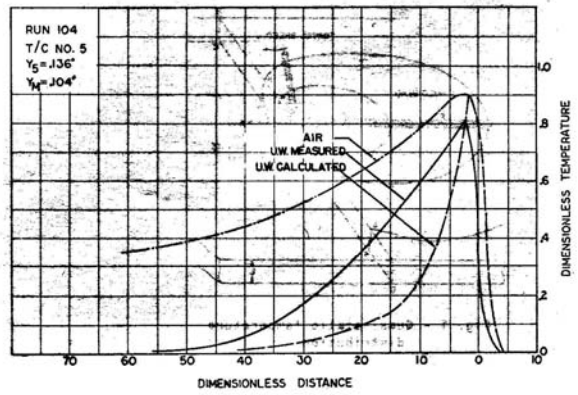

Fig. 7 - Temperature comparison curves.

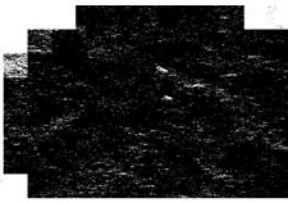

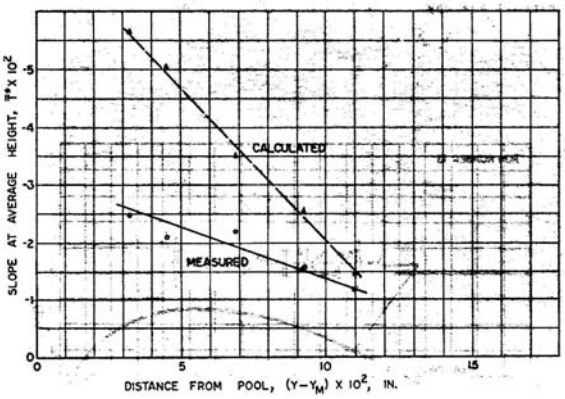

Fig. 8 - Comparison of cooling curve slopes.

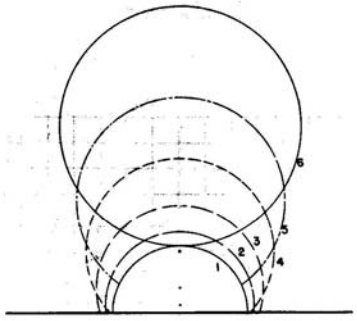

Fig. 9 - Idealized bubble dynamics and breakaway.